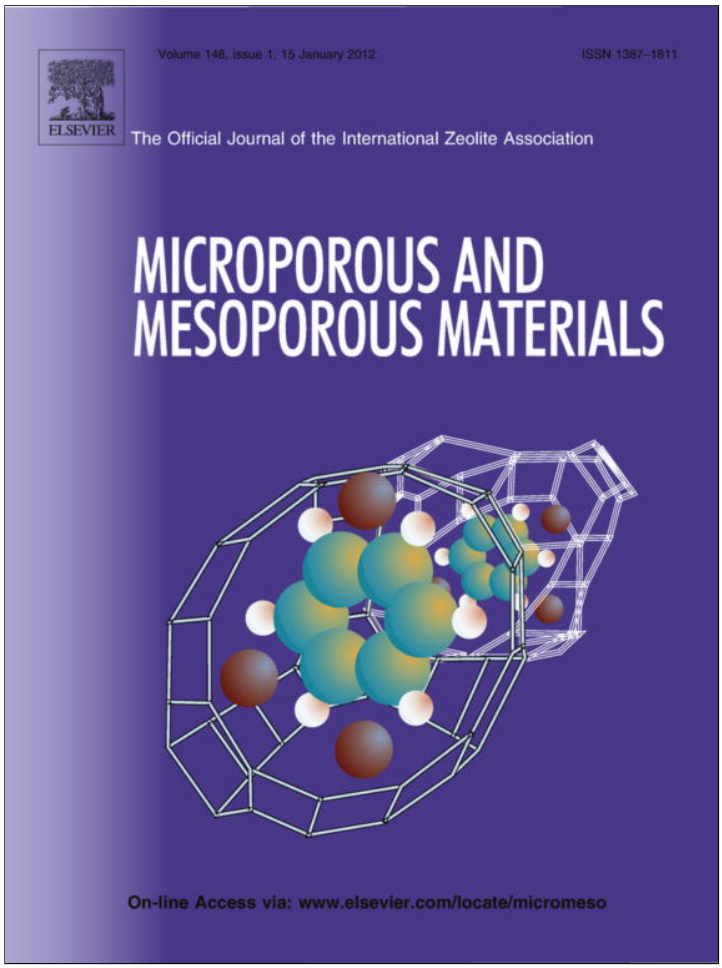

Microporous and Mesoporous Materials 148 (2012) 184–190

Contents lists available at SciVerse ScienceDirect

Microporous and Mesoporous Materials

journal homepage: www.elsevier.com/locate/micromeso

Nitridation of MgO-loaded MCM-41 and its beneficial applications in base-catalyzed reactions

Tao Wang, Guangjun Wu, Naijia Guan, Landong Li *

Key Lab of Advanced Energy Materials Chemistry (Ministry of Education), College of Chemistry, Nankai University, Tianjin 300071, PR China

ARTICLE INFO

Article history:
Received 2 March 2011
Received in revised form 2 June 2011
Accepted 10 July 2011
Available online 18 August 2011

Keywords:
MgO-MCM-41
Nitridation
Basicity
Base-catalyzed reaction

ABSTRACT

Nitrogen-containing MgO-MCM-41 solid base material is prepared by nitridation of MgO-loaded mesoporous MCM-41. The ordered mesoporous structure and high surface area of MCM-41 are well preserved after MgO impregnation and nitridation, as proved by the XRD, TEM and nitrogen adsorption/desorption analysis. FTIR spectra the bridging –NH– groups and terminal $–NH_2$ groups are incorporated into the framework of MgO-MCM-41 by nitridation, and the base strength is expected to be enhanced due to the replacement of oxygen by nitrogen with lower electronegativity. FTIR spectra with the adsorption of different probe molecules, e.g. CO, CD_3CN and $^{13}CO_2$, are employed for the characterization of surface acidic–basic properties of MgO-MCM-41 before and after nitridation. It is revealed that the acidic hydroxyls in MgO-MCM-41 are greatly reduced through nitridation process. Compared with MgO-MCM-41, the nitridized MgO-MCM-41 material exhibits improved basic catalytic performances in Knoevenagel condensation reaction, Claisen–Schmidt reaction and dehydrogenation reaction of 2-propanol.

1. Introduction

The replacement of liquid bases by solid bases as catalysts has attracted much attention due to the easy separation from the products, as well as possible regeneration and reuse [1]. Solid base materials can exhibit good activities and high selectivity in many base-catalyzed reactions, with the advantages of being noncorrosive and environmentally friendly [2]. A number of materials have been reported to act as solid base catalysts, including but not limited to single component metal oxides, zeolites, supported alkali metal ions and clay minerals [3]. However, the search of promising solid bases that can catalyze reactions with high activities and selectivity is still an ongoing process.

Mesoporous molecular sieves, such as MCM-41 and SBA-15, may serve as idea supports for solid bases due to their tunable large pores and high surface areas [4]. It has been reported that template-containing mesoporous molecular sieves, e.g. MCM-41 and MCM-48, show peculiar basicity due to the presence of siloxy anions and CTA^+ cations [5]. These materials exhibit good activity in base-catalyzed reactions at relatively low temperatures though the partial leaching of organic cations is observed at the beginning of reaction [6]. Generally, alkaline-earth metal oxides, e.g. MgO, CaO and BaO, can be deposited on mesoporous molecular sieves to prepare supported solid bases with high surface area and good stability [7–11]. While the base strength of alkaline-earth metal oxides may decrease due to the interaction between alkaline-earth metal oxides and the mesoporous supports. Moreover, the abundant surface hydroxyls of mesoporous supports will bring many by-products in base-catalyzed reactions.

Recently, nitridation has been employed as an effective method to prepare basic mesoporous catalytic materials. The oxygen atoms of framework are replaced to some level by certain isoelectronic groups, e.g. –NH– species. The Lewis basicity is enhanced due to the lower electronegativity of nitrogen with respect to oxygen [12]. The porous structures and high specific surface areas of parent materials can be well preserved after nitridation under proper conditions. Various nitrogen-incorporated mesoporous molecular sieves, e.g. FSM-16 [13], MCM-41 [14–16], SBA-15 [17,18] and MCM-48 [19,20], have been successfully prepared. However, the application of nitrogen-incorporated mesoporous molecular sieves is confined to Knoevenagel condensation reaction, a typical base-catalyzed probe reaction. The basicity of nitridized mesoporous molecular sieves is not strong enough for most other base-catalyzed reactions.

In this work, promising strong solid base catalysts are prepared by nitridation of MgO-loaded mesoporous MCM-41. The base strength of as-prepared materials is enhanced by nitridation to some extent, while the surface hydroxyls of mesoporous MCM-41 are replaced by terminal $–NH_2$ groups [21]. FTIR spectra with different probe molecules are employed to analyze the physicochemical properties of as-prepared materials. Several typical base-catalyzed reactions, e.g. Knoevenagel condensation reaction, Claisen–Schmidt reaction and conversion of 2-propanol, are employed for the evaluation of basicity of as-prepared materials.

* Corresponding author. Tel./fax: +86 22 2350 0341.
E-mail address: lild@nankai.edu.cn (L. Li).

1387-1811/$ - see front matter © 2011 Elsevier Inc. All rights reserved.
doi:10.1016/j.micromeso.2011.07.024

2. Experiment

2.1. Catalysts preparation

All-silica MCM-41 was synthesized according to the literature report [22] and MgO-MCM-41 was prepared by wet impregnation using MCM-41 as support. Typically, a mixture containing 2.0 g of calcined all-silica MCM-41, 1.2 g of $Mg(CH_3COO)_2{\cdot}4H_2O$ and 100 ml of deionized water were mixed and stirred at room temperature for 4 h. The sample was dried at 80 °C for 12 h, calcined at 550 °C for 4 h and labeled as MgO-MCM-41.

For the nitridation of MgO-MCM-41, 1.0 g of as-prepared MgO-MCM-41 was placed in a quartz boat and treated with NH_3 flow (99.0% purity) at 800 °C for 12 h. The NH_3 flow rate was 400 ml/min and the heating rate was 2 °C/min. The material after nitridation was labeled as MgO-MCM-41-N. The total nitrogen content in MgO-MCM-41-N is determined to be 4.68 wt.% by CHN analysis and the Mg content is determined to be 5.32% by ICP analysis.

2.2. Catalysts characterization

Powder X-ray diffraction patterns of samples were collected on a D/Max-2500 powder diffractometer (36 kV and 20 mA) using Cu-Kα (λ = 1.54178 Å) radiation.

Nitrogen adsorption/desorption measurements of samples were performed at −196 °C on a NOVA 1000e (Quantachrome Instruments) after outgassing at 300 °C under vacuum for 12 h.

Transmission electron microscopy (TEM) images were taken on a Philips Tecnai G^2 20 S-TWIN electron microscope at an accelerate voltage of 200 kV. A few drops of alcohol suspension containing the sample were placed on a carbon-coated copper grid, followed by evaporation at ambient temperature.

FTIR spectra of the samples were measured on a Bruker Tensor 27 spectrometer with a liquid N_2 cooled high sensitivity MCT detector. FTIR spectra with probe adsorption (CO, CD_3CN or CO_2) were performed on the spectrometer using a reaction chamber connected to a vacuum adsorption system with a base pressure below 10^{-3} Pa. The self-supporting wafers of samples (*ca.* 20 mg) were pretreated in oxygen at 300 °C and then evacuated at the same temperature to remove contaminations and adsorbed water. After cooling to room temperature in vacuum, the samples were exposed to probe molecular at room temperature and FTIR spectra were recorded with 128 single beam spectra co-added at a resolution of 4 cm^{-1}.

2.3. Catalytic activity evaluation

The as-prepared materials were evaluated as catalysts for Knoevenagel condensation reaction, Claisen–Schmidt reaction and dehydrogenation reaction of 2-propanol.

Knoevenagel condensation reaction: benzaldehyde (40.0 mmol), malononitrile (40.0 mmol) and toluene (10.0 ml) were mixed in a three-necked bottom flask with a condenser system. The mixture heated to the temperature of 80 °C in a water bath under stirring, 0.15 g of catalyst was then added into the flask. The progress of the reaction was monitored by periodically withdrawing 0.2 μl of liquid samples with a filtering syringe. The reactants and products were analyzed by GC-7890F gas chromatograph equipped with a FID and a 0.20 mm × 50 m FFAP capillary column.

Claisen–Schmidt reaction: benzaldehyde (2.5 mmol), acetophenone (3.0 mmol) and toluene (3.0 ml) were mixed in a three-necked bottom flask with a condenser system. The mixture heated to the temperature of 80 °C in a water bath under stirring, 0.15 g of catalyst was then added into the flask. The progress of the reaction was monitored by periodically withdrawing 0.2 μl of liquid samples with a filtering syringe. The reactants and products were analyzed by GC-7890F gas chromatograph equipped with a FID and a 0.20 mm × 50 m FFAP capillary column.

Dehydrogenation reaction of 2-propanol: the reaction was carried out on a fixed-bed microreactor at atmospheric pressure. About 0.2 g of the catalyst (mesh of 20–40) was placed in the isothermal region of the reactor. 2-Propanol was fed into the reactor by a syringe infusion pump at the flow rate of 0.4 ml/h. The reactor was heated to the desired temperature. After reaction for 1 h, the product was analyzed on line by a SP-502 gas chromatograph, equipped with a FID and a 4 mm × 3 m packed column.

3. Results and discussion

3.1. Physico-chemical properties of samples

The X-ray diffraction patterns of MgO-MCM-41 before and after nitridation are presented in Fig. 1. For MgO-MCM-41, an intense (1 0 0) diffraction peak (2θ = 2.1°), together with weak (1 1 0) diffraction peak (2θ = 3.6°) and weak (2 0 0) diffraction peak (2θ = 4.2°), is clearly observed, corresponding to the characteristic MCM-41 structure. After nitridation at 800 °C, the intensities of (1 1 0) and (2 0 0) peaks decrease a little. The characteristic hexagonal structures of MCM-41 are well preserved in MgO-MCM-41 after nitridation. It is also seen that no peaks corresponding to MgO species can be observed on the XRD patterns of MgO-MCM-41 and MgO-MCM-41-N, indicating a good dispersion of MgO species on MCM-41 support.

Fig. 2 shows the N_2 adsorption–desorption isotherms of MCM-41, MgO-MCM-41 and MgO-MCM-41-N. All samples exhibit type IV adsorption curves, which are characteristic of mesoporous materials [23]. The hysteresis loop in the region of P/P_0 above 0.4 is observed and such hysteresis should be assigned to the capillary condensation in the mesopores [24]. The highly ordered mesoporous structure of MCM-41 is preserved after loading of MgO and nitridation. While the partially block of mesopores in MgO-MCM-41 and MgO-MCM-41-N can be deduced by comparison between the BJH plots obtained from the desorption branch and those from the adsorption branch [25,26]. The textural properties of samples derived from N_2 sorption isotherms are summarized in Table 1. It is seen that the BET surface area and pore volume of MCM-41 decrease distinctly after loading of MgO. While the average pore size of MCM-41 increases slightly due to the expanding of mesoporosity of MCM-41 by the gas produced from calcination of precursor $Mg(CH_3COO)_2{\cdot}4H_2O$. After nitridation, the BET surface area and pore volume further decreases, probably due to the aggregation of MgO during nitridation process at elevated temperature. Nevertheless, the ordered mesoporous structure of parent MCM-41 are preserved after loading of MgO and nitridation, as supported by the XRD patterns and TEM observations (Fig. 3).

FTIR spectroscopy is frequently used to determine the surface groups formed by nitridation [27] and the FTIR spectra of MgO-MCM-41 before and after nitridation are presented in Fig. 4. The strong band at 3740 cm^{-1} assignable to the O–H vibration of Si–OH groups can be observed on MgO-MCM-41 and MgO-MCM-41-N catalysts. For MgO-MCM-41-N, strong band at 3380 cm^{-1} assignable to the N–H asymmetric vibration of bridging –NH– groups [14,18], as well as very weak band at 1550 cm^{-1} assignable to the symmetric bending vibration of terminal $–NH_2$ groups [20], appears. The results from FTIR spectroscopy unambiguously confirm the substitution of oxygen in the framework by NH after nitridation, leading to the formation of basic bridging –NH– and terminal $–NH_2$ species. Moreover, it is indicated that NH prefers to replace oxygen atom in

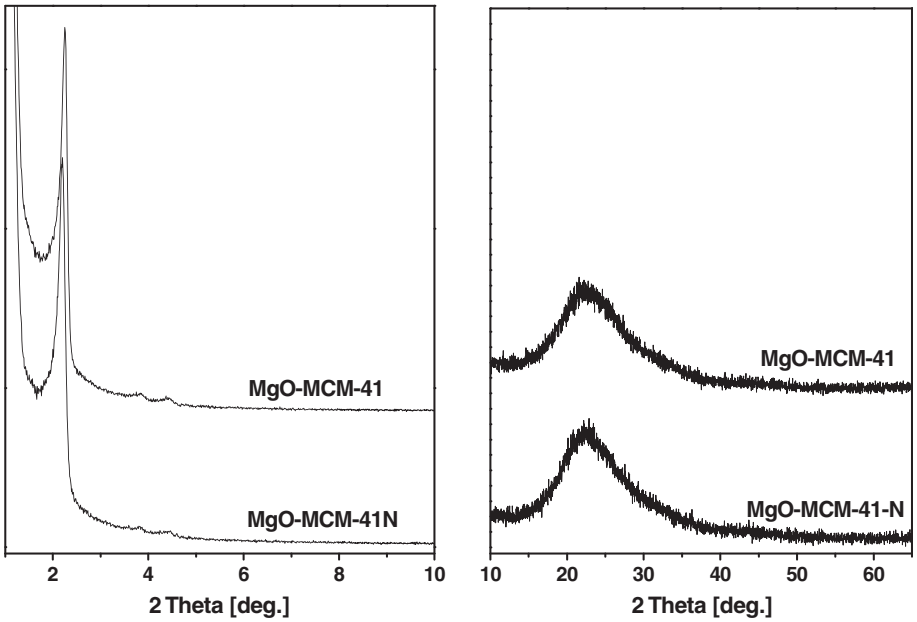

Fig. 1. X-ray diffraction patterns of MgO-MCM-41 before and after nitridation.

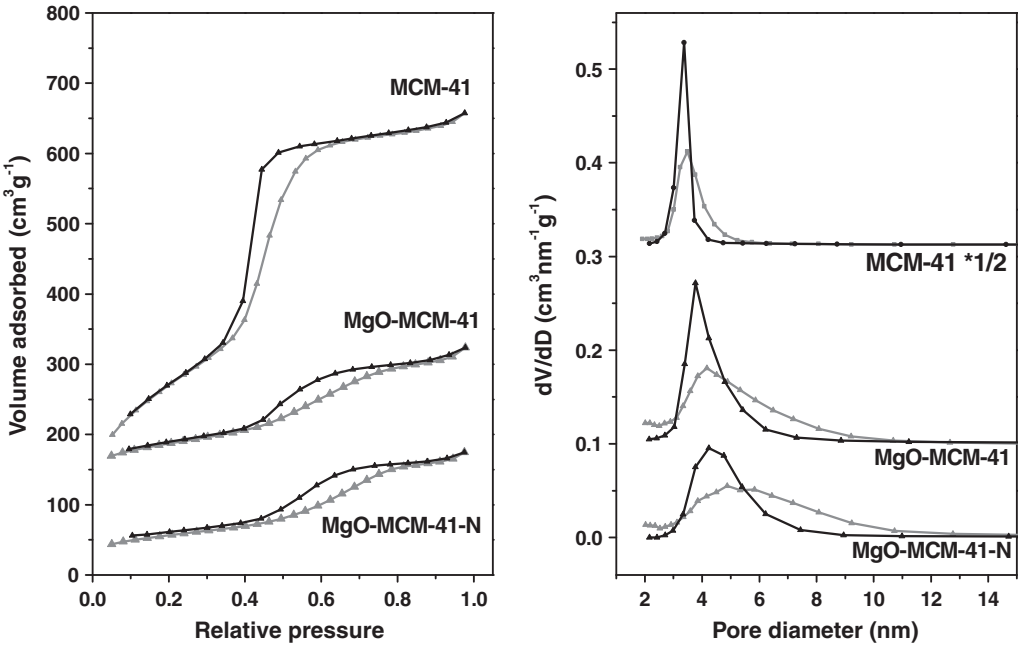

Fig. 2. Nitrogen sorption isotherms and mesopore size distribution of MCM-41, MgO-MCM-41 and MgO-MCM-41-N.

Table 1
Textural properties of MCM-41 and MgO-MCM-41 before and after nitridation.

Samples	S_{BET} [a] (m^2/g)	Average pore diameter (nm)	Pore volume (cm^3/g)
MCM-41	953	4.27	1.02
MgO-MCM-41	289	4.78	0.34
MgO-MCM-41-N	191	5.65	0.27

[a] Calculated by DFT method.

Si–O–Si rather than that in Si–OH, and consequently bridging –NH– species are the main basic species created by nitridation.

Carbon monoxide (CO) is frequently used probe molecule for determination of surface basicity [28]. Fig. 5 shows FTIR spectra of CO adsorption on MgO-MCM-41 before and after nitridation. The bands at 1660 and 1280 cm^{-1}, corresponding to ν(C=O) and ν_{as}(COO) of carbonates [29,30], are observed on both MgO-MCM-41 and MgO-MCM-41-N. The band at 1350 cm^{-1} corresponding to the ν_s(COO–) of formates [31] is observed on MgO-MCM-41, while it disappears after nitridation. It is known that the formates are formed from CO adsorption on reactive surface hydroxyls. The disappearance of band at 1350 cm^{-1} clearly indicates the removal of reactive surface hydroxyls after nitridation, which is essential for the catalytic application.

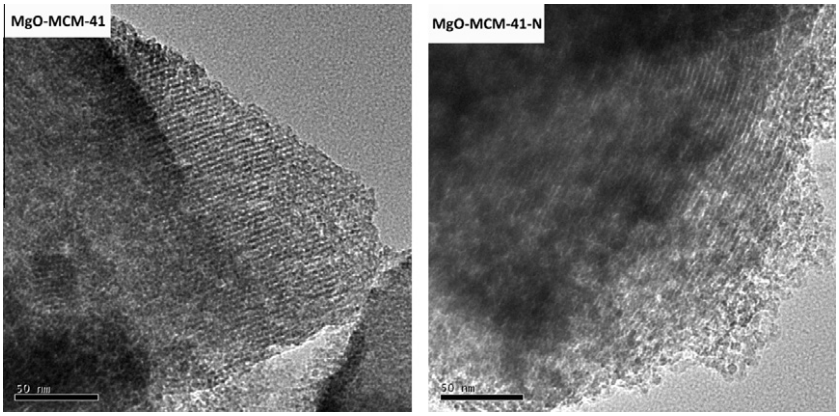

Fig. 3. TEM images of MgO-MCM-41 and MgO-MCM-41-N.

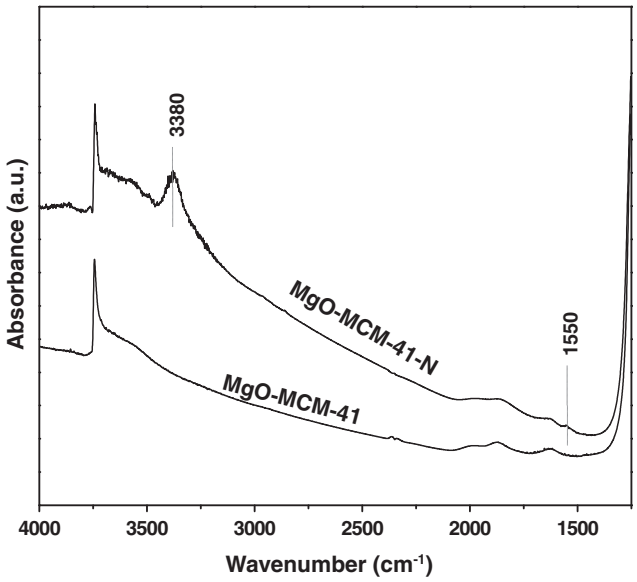

Fig. 4. FTIR spectra of MgO-MCM-41 before and after nitridation at 800 °C.

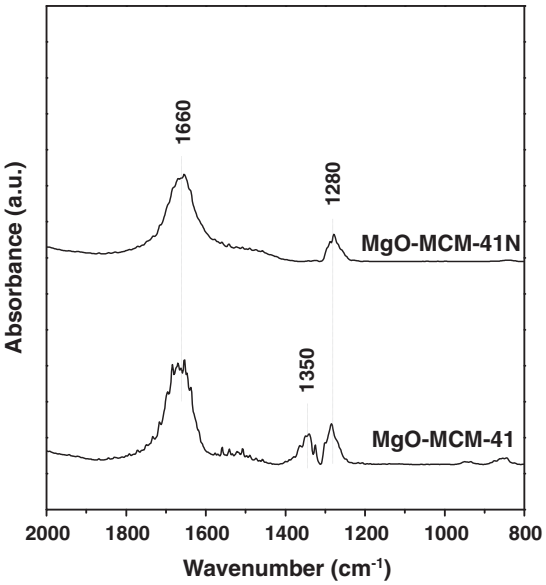

Fig. 5. FTIR spectra of CO adsorption for MgO-MCM-41 before and after nitridation.

The acidity of the MgO-MCM-41 before and after nitridation is investigated by FTIR using deuterated acetonitrile (CD_3CN) as a probe molecule. As seen in Fig. 6, bands at 2300, 2270, 2115 and 1660 cm^{-1} appear upon CD_3CN adsorption on MgO-MCM-41. The band at 2110 cm^{-1} is due to the $\delta_s(CD_3)$ of physisorbed CD_3CN on sample [32]. The bands at 2270 and 2300 cm^{-1} are assigned to ν (CN) of chemisorbed CD_3CN on different Lewis acid sites [33]. The band at 1660 cm^{-1} is due to the strong H complex formed between basic CD_3CN molecules and acidic surface hydroxyls [32]. As for MgO-MCM-41-N, the bands at 2270 and 2300 cm^{-1} are observed upon CD_3CN adsorption and their intensities are quite similar to those on MgO-MCM-41, indicating that the Lewis acid are preserved after nitridation. In contrast, the intensity of IR band at 1660 cm^{-1} caused by CD_3CN adsorption on MgO-MCM-41-N decreases dramatically compared to that on MgO-MCM-41. Obviously, the acidic hydroxyls are greatly reduced through nitridation process.

Acidic carbon dioxide (CO_2) is good probe for the characterization of solid base catalysts. Spectroscopic studies show that CO_2 may adsorb over surface basic oxygen sites and Lewis acid sites [34]. CO_2 strongly interacts with basic oxygen site to form carbonate-like species and the surface structures including basic sites can be estimated from the adsorbed states of CO_2 [3], illustrated by the IR bands in the range of 1300–1700 cm^{-1}. Over Lewis acid sites, CO_2 adsorbs in a linear configuration and the main IR bands are in the range of 2200–2400 cm^{-1}. Since the IR bands originated from adsorption of $^{12}CO_2$ on supported alkaline metal oxides are usually disturbed by the presence of $^{13}CO_2$ [35], $^{13}CO_2$ (99.0%) is employed in our experiments for a better distinguishment of IR bands formed.

Fig. 7 shows the IR spectra of $^{13}CO_2$ adsorbed on MgO-MCM-41 before and after nitridation. In the IR region of linear $^{13}CO_2$ adsorption, two intense bands are observed at 2290 and 2280 cm^{-1}. The former is attributed to $^{13}CO_2$ on Mg^{2+} cations [36], and the latter is attributed to the ν_3 mode of $^{13}CO_2$ [37]. After nitridation, the intensity of band at 2290 cm^{-1} decreases distinctly, indicating that the accessibility of Mg^{2+} cation sites decreases to some extent after nitridation. After evacuated at room temperature for 1 h, the bands originated from linear $^{13}CO_2$ adsorption disappear due to the remove of weakly adsorbed $^{13}CO_2$.

In the IR region of 1300–1700 cm^{-1}, bands at 1630, 1405 and 1370 cm^{-1} can be observed on MgO-MCM-41. The high-frequency band at 1630 cm^{-1} is assigned to the assigned to $\nu_{as}(COO)$ of bicarbonate and the band at 1405 cm^{-1} is assigned to the $\nu_s(COO)$ of bicarbonate [38,39]. The band at 1370 cm^{-1} is assigned to the $\nu_s(COO)$ of bidentate carbonate [39], while the corresponding asymmetric vibration at *ca.* 1590 cm^{-1} is hard to distinguish due

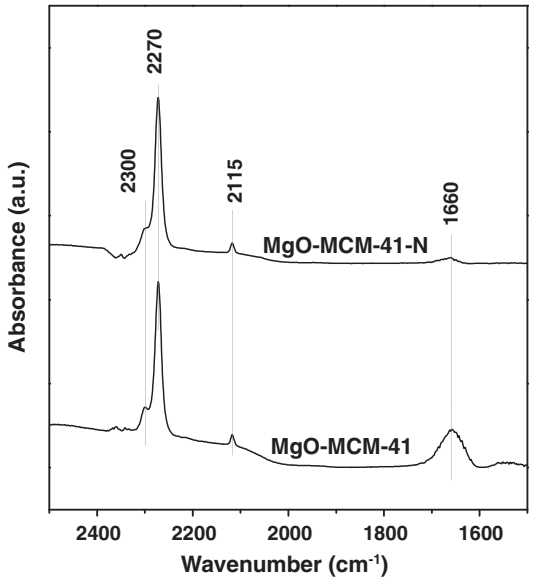

Fig. 6. FTIR spectra of CD_3CN adsorption for MgO-MCM-41 before and after nitridation.

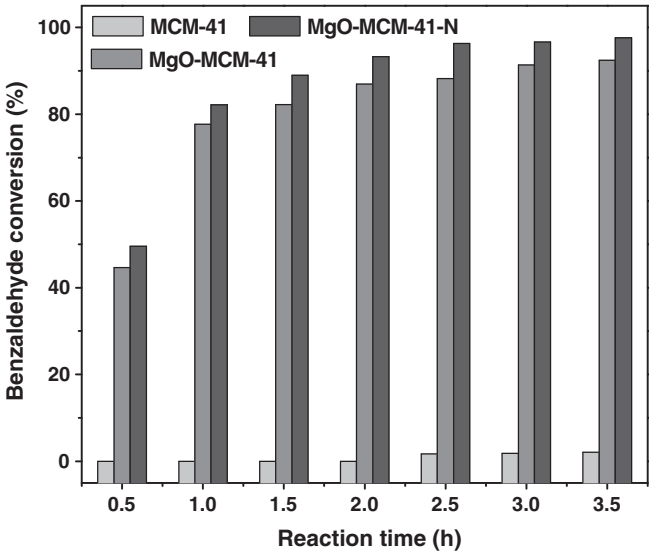

Fig. 8. Knoevenagal condensation reaction of benzaldehyde and malononitrile over MCM-41, MgO-MCM-41 and MgO-MCM-41-N.

to the overlap by the strong band at 1630 cm^{-1}. After evacuation at room temperature, an obvious decrease in the intensity of these IR bands is observed, indicating the poor stability of formed species. For MgO-MCM-41-N, much less bicarbonate species are formed upon CO_2 adsorption, as illustrated by the lower intensity of corresponding IR bands at 1405 and 1630 cm^{-1}. Meanwhile, no bidentate carbonate species are formed upon CO_2 adsorption. Through nitridation, parts of surface oxygen atoms are replaced by nitrogen atoms (–NH), which hinders the formation of carbonate and bicarbonate species. However, the formed bicarbonate species on MgO-MCM-41-N exhibits better stability than those on MgO-MCM-41, indicating the better stability of basic sites on MgO-MCM-41-N than those on MgO-MCM-41. The stability of basic sites is essential for the application in base-catalyzed reactions at elevated temperatures.

3.2. Catalytic performances

3.2.1. Knoevenagel condensation reaction

Knoevenagel condensation reaction is one of the reactions used for carbon–carbon bond formation and has been widely used for the commercial preparation of fine chemistry intermediates [40]. This reaction is also extensively employed as model reaction for the evaluation of solid base catalysts. We perform Knoevenagel condensation reaction between benzaldehyde and malononitrile to evaluate the basicity of as-prepared materials under mild conditions and the catalytic results are shown in Fig. 8. All-silica MCM-41 shows negligible activity in the reaction due to the absence of any basic center on the surface [14]. MgO-MCM-41 shows good activity for Knoevenagel condensation reaction because the relatively strong basic center introduced after the impregnation of MgO. The conversion of benzaldehyde is *ca.*

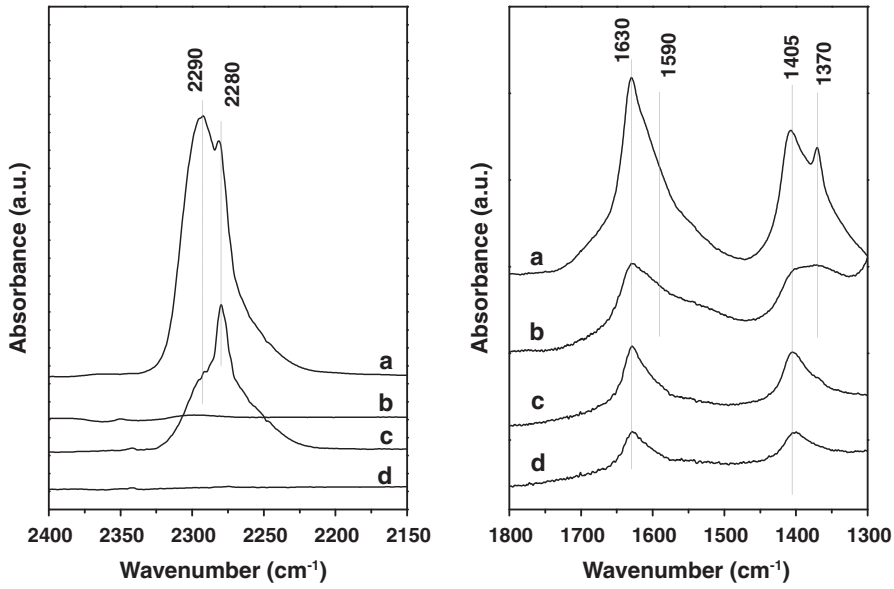

Fig. 7. FTIR spectra of (a) $^{13}CO_2$ on MgO-MCM-41 pre-evacuated at 300 °C for 2 h, (b) sample (a) evacuated at RT for 1 h, (c) $^{13}CO_2$ on MgO-MCM-41-N pre-evacuated at 300 °C for 2 h and (d) sample (c) evacuated at RT for 1 h.

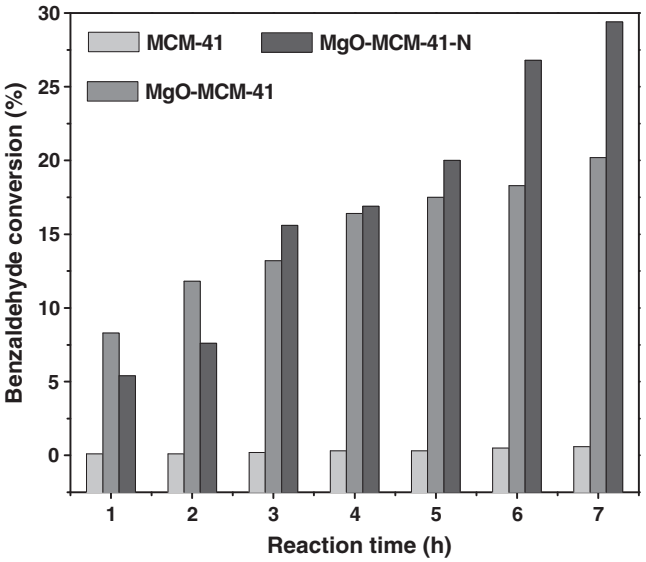

Fig. 9. Claisen–Schmidt reaction of benzaldehyde and acetophenone over MCM-41, MgO-MCM-41 and MgO-MCM-41-N.

93.3% over MgO-MCM-41 after reaction for 4 h. After nitridation, the basic catalytic activity for Knoevenagel condensation reaction is obviously promoted. The conversion of benzaldehyde over MgO-MCM-41-N can reach up to *ca.* 98.5% after reaction for 4 h, suggesting that the basicity of MgO-MCM-41 increases to some extent after proper nitridation. The selectivity to target product 1,1-dicyanophenylethylene is approaching 100%. No further reaction such as the Michael addition reaction, which involves the reaction of 1,1-dicyanophenylethylene with another malononitrile molecule, can be detected under our reaction conditions.

3.2.2. Claisen–Schmidt condensation reaction

Claisen–Schmidt condensation reaction is the most frequently used for carbon–carbon bond formation in the organic synthesis of chalcones, which represent one of the most rich and omnipresent groups of natural products [41]. In recent years, chalcones have been shown to possess interesting biological properties and can be used as synthetic intermediates in the preparation of several important compounds. Claisen–Schmidt condensation of benzaldehyde with acetophenone is performed for the evaluation of the basicity of as-prepared materials under mild conditions and the catalytic results are shown in Fig. 9. Basic center with certain strength is required to promote the formation of carbanions, which are the important intermediates in the reaction. The absence of basic center makes all-silica MCM-41 show negligible activity in Claisen–Schmidt condensation reaction. After the impregnation of MgO, MgO-MCM-41 exhibits certain activity and the conversion of benzaldehyde can reach *ca.* 20.2% after reaction for 7 h. Because acetophenone (p*K*a = 19.1) is less reactive than malononitrile (p*K*a = 11.2), MgO-MCM-41 exhibits lower activity for Claisen–Schmidt condensation in comparison to Knoevenagel condensation under similar conditions. After nitridation, the catalytic activity of MgO-MCM-41 for Claisen–Schmidt condensation reaction is promoted to some extent and the conversion of benzaldehyde over MgO-MCM-41-N can reach up to *ca.* 29.4% after reaction for 7 h. The selectivity to target product chalcone is close to 100% over all catalysts studied. Neither benzyl alcohol nor benzoic acid can be detected in the reaction products, indicating that the Cannizaro reaction does not take place under our reaction conditions.

3.2.3. Conversion of 2-propanol

The conversion of 2-propanol is recognized as popular model reaction for the characterization of acid and base sites of solid catalysts. The 2-propanol may dehydrate to propene on acid sites or dehydrogenate to acetone on base sites. The conversion of 2-propanol to acetone is employed to determine the basic properties of MgO-MCM-41 before and after nitridation. Fig. 10 shows the results of 2-propanol conversion over MgO-MCM-41 and MgO-MCM-41-N. No other products except acetone and propene can be detected under our reaction conditions. MgO-MCM-41 shows high activity for 2-propanol conversion than MgO-MCM-41-N at <400 °C. At temperature of >400 °C, 2-propanol conversion of 100% is obtained on both catalysts. Since 2-propanol conversion can be catalyzed by acidic sites or basic sites, the lower activity of MgO-MCM-41-N at <400 °C is ascribed to the reduction of acid sites through nitridation, as proved by FTIR results. For MgO-MCM-41, the selectivity to acetone is very low and the maximal yield of acetone is observed to be *ca.* 5.4% at the reaction temperature is 450 °C. The main reaction product is propene from the

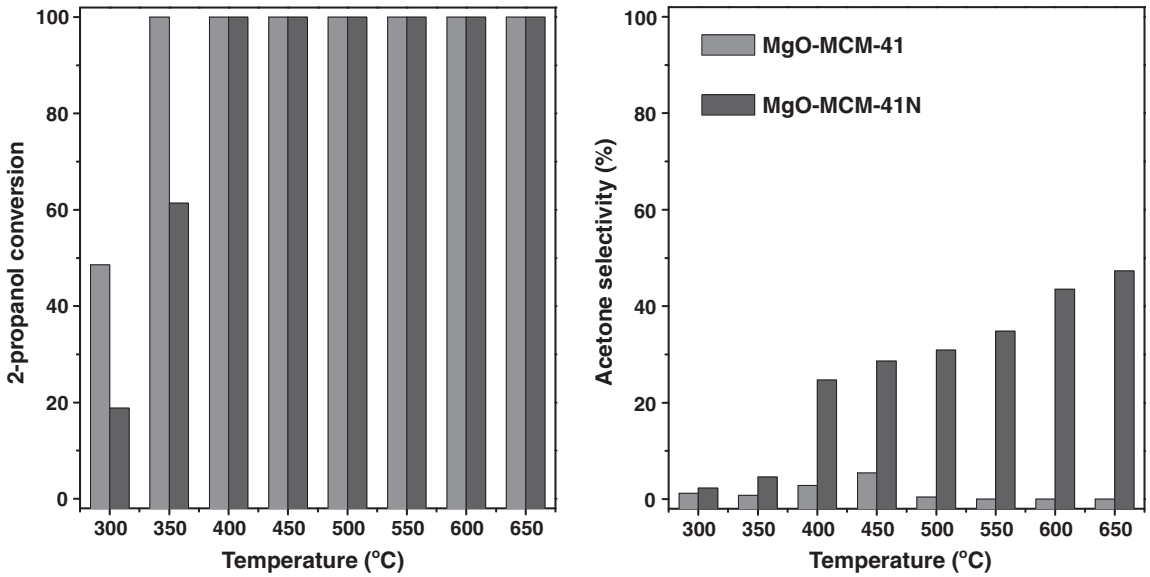

Fig. 10. 2-Propanol dehydrogenation reaction over MgO-MCM-41 and MgO-MCM-41-N.

dehydration of 2-propanol catalyzed by the acidic surface hydroxyls. After nitridation, the selectivity to acetone greatly enhanced and a maximal acetone yield of *ca.* 47.3% can be observed at the reaction temperature of 650 °C. The reduction of acidic sites through nitridation suppresses the route of 2-propanol dehydration to propene, and thus promotes the route of 2-propanol dehydrogenation to acetone.

4. Conclusions

Promising solid base catalyst MgO-MCM-41-N is prepared by nitridation of MgO-loaded mesoporous MCM-41. After MgO impregnation and nitridation, the ordered mesoporous structure and high surface area of MCM-41 are well preserved. Basic species, bridging –NH– and terminal $–NH_2$ groups, are introduced into the framework of MgO-MCM-41 by nitridation, as illustrated by FTIR spectra. Correspondingly, MgO-MCM-41-N shows improved activity than parent MgO-MCM-41 in two typical base-catalyzed reactions, e.g. Knoevenagel condensation reaction and Claisen–Schmidt reaction. FTIR spectra with adsorption of probe molecules, e.g. CO, CD_3CN and $^{13}CO_2$, reveal that the acidic hydroxyls in parent MgO-MCM-41 can be greatly reduced through nitridation. Since pure solid bases without acidic sites do not exist [42], nitridation can act as effective tool to reduce acidic sites in solid bases. In this work, MgO-MCM-41-N shows improved 2-propanol dehydrogenation selectivity to acetone than MgO-MCM-41 due to the reduction of acidic hydroxyls, which contribute to the 2-propanol dehydration to propene.

Acknowledgements

We greatly thank Prof. Helmut Knözinger and Dr. Mihail Mihaylov for the IR characterization. This work was supported by National Basic Research Program of China (973 Program 2009CB623502) and MOE (IRT0927).

References

[1] Y. Ono, T. Baba, Catal. Today 38 (1997) 321–337.
[2] R.J. Davis, J. Catal. 216 (2003) 396–405.
[3] H. Hattori, Chem. Rev. 95 (1995) 537–558.
[4] Y. Ono, J. Catal. 216 (2003) 406–415.
[5] D.P. Fabiano, B. Hamad, D. Cardoso, N. Essayem, J. Catal. 276 (2010) 190–196.
[6] L. Martins, W. Höderich, P. Hammer, D. Cardoso, J. Catal. 271 (2010) 220–227.
[7] J.I. Yu, S.Y. Shiau, A.N. Ko, Catal. Lett. 77 (2001) 165–169.
[8] S. Jaenicke, G.K. Chuah, X.H. Lin, X.C. Hu, Micropor. Mesopor. Mater. 35–36 (2000) 143–153.
[9] J.O. Barth, A. Jentys, J. Kornatowski, J.A. Lercher, Chem. Mater. 16 (2004) 724–730.
[10] Q. Li, S.E. Brown, L.J. Broadbelt, J. Zheng, N. Wu, Micropor. Mesopor. Mater. 59 (2003) 105–111.
[11] Y. Wei, Y. Cao, J. Zhu, X. Yan, Chin. J. Inorg. Chem. 19 (2003) 233–239.
[12] J. Xiong, Y. Ding, L. Lin, J. Phys. Chem. B 107 (2003) 1366–1369.
[13] Y. Inaki, Y. Kajita, H. Yoshida, K. Ito, T. Hattori, Chem. Commun. (2001) 2358–2359.
[14] Y. Xia, R. Mokaya, J. Mater. Chem. 14 (2004) 2507–2515.
[15] C. Zhang, Q. Liu, Z. Xu, J. Non-Cryst. Solids 351 (2005) 1377–1382.
[16] S. Jiang, Y. Song, F. Zhang, G. Wu, N. Guan, Chin. J. Catal. 27 (2006) 495–500.
[17] N. Chino, T. Okubo, Micropor. Mesopor. Mater. 87 (2005) 15–22.
[18] J. Wang, Q. Liu, Micropor. Mesopor. Mater. 83 (2005) 225–232.
[19] Y. Xia, R. Mokaya, Angew. Chem. Int. Ed. 42 (2003) 2639–2644.
[20] Y. Xia, R. Mokaya, J. Phys. Chem. C 112 (2008) 1455–1462.
[21] S. Ernst, M. Hartmann, S. Sauerbeck, T. Bongers, Appl. Catal. A 200 (2000) 117–123.
[22] C.T. Kresge, M.E. Leonowicz, W.J. Roth, J.C. Vartuli, J.S. Beck, Nature 359 (1992) 710–712.
[23] C. Chen, H. Li, M.E. Davis, Micropor. Mater. 2 (1993) 17–26.
[24] S.J. Gregg, K.S.W. Sing, Adsorption, Surface Area and Porosity, Academic Press, London, 1982.
[25] J.C. Groen, J. Pérez-Ramírez, Appl. Catal. A 268 (2004) 121–125.
[26] J.C. Groen, L.A.A. Peffer, J. Pérez-Ramírez, Micropor. Mesopor. Mater. 60 (2003) 1–17.
[27] K.D. Hammond, M. Gharibeh, G.A. Tompsett, F. Dogan, A.V. Brown, C.P. Grey, S.M. Auerbach, W.C. Conner, Chem. Mater. 22 (2010) 130–142.
[28] K.I. Hadjiivanov, G.N. Vayssilov, Adv. Catal. 47 (2002) 307–511.
[29] W. Zhang, Z. Huang, S. Liao, F. Cui, J. Am. Ceram. Soc. 86 (2003) 1052–1054.
[30] C. Schild, A. Wokaun, J. Mol. Catal. 63 (1990) 223–242.
[31] M. Kantcheva, M.U. Kucukkal, S. Suzer, J. Catal. 190 (2000) 144–156.
[32] A.G. Pelmenschikov, R.A. van Santen, J. Janchen, E. Meijer, J. Phys. Chem. 97 (1993) 11071–11074.
[33] J. Chen, J.M. Thomas, G. Sankar, J. Chem. Soc. Faraday Trans. 90 (1994) 3455–3459.
[34] G. Busca, V. Lorenzelli, Mater. Chem. 7 (1982) 89–126.
[35] G. Wu, S. Jiang, L. Li, N. Guan, Appl. Catal. A 391 (2011) 225–233.
[36] M. Pohl, A. Otto, Surf. Sci. 406 (1998) 125–137.
[37] B. Bonelli, B. Civalleri, B. Fubini, P. Ugliengo, C.O. Areán, E. Garrone, J. Phys. Chem. B 104 (2000) 10978–10988.
[38] H.A. Prescott, Z. Li, E. Kemnitz, A. Trunschke, J. Deutsch, H. Lieske, A. Auroux, J. Catal. 234 (2005) 119–130.
[39] G.A.H. Mekhemer, S.A. Halawy, M.A. Mohamed, M.I. Zaki, J. Phys. Chem. B 108 (2004) 13379–13386.
[40] G. Marciniak, A. Delgado, G. Leclerc, J. Velly, N. Decker, J. Schwartz, J. Med. Chem. 32 (1989) 1402–1407.
[41] M.J. Climent, A. Corma, S. Iborra, A. Velty, J. Catal. 221 (2004) 474–482.
[42] G. Busca, Chem. Rev. 110 (2010) 2217–2249.